Cement and Concrete Research 41 (2011) 947–954

Contents lists available at ScienceDirect

Cement and Concrete Research

journal homepage: http://ees.elsevier.com/CEMCON/default.asp

Alternative blended cement with ceramic residues: Corrosion resistance investigation on reinforced mortar

Maria Chiara Bignozzi *, Stefano Bonduà

Dipartimento di Ingegneria Civile, Ambientale e dei Materiali, Università di Bologna, Via Terracini 28, 40131 Bologna, Italy

ARTICLE INFO

Article history:
Received 23 September 2010
Accepted 3 May 2011

Keywords:
Blended cement (D)
Corrosion (C)
Pore size distribution (B)
Microstructure
Durability

ABSTRACT

Blended cements are largely used for concrete: they are usually considered cements with a low environmental impact, as they require less clinker than ordinary Portland cement (OPC). Different constituents can be used as supplementary clinker component usually leading to cement with high resistance to outdoor environment. Polishing residue (PR), coming from porcelain stoneware tiles production, can be successfully used as new constituent for blended cement, however its action for enhancing the durability of cement matrix must be assessed. With this purpose, electrochemical tests (half cell potential, impressed voltage and linear polarization techniques) have been carried out on steel reinforced mortar samples, prepared using a 25% PR based cement and 100% OPC as binder and exposed to a 3.5% NaCl solution. The corrosion resistance results and microstructure analysis highlight better durability performances for PR based cement than those exhibited by OPC, mainly for curing time >28 days.

1. Introduction

The use of blended cements is growing very fast as a consequence of the massive energy consumption and large CO_2 emissions released throughout Portland cement clinker production. Blended cements include all the cements where Portland cement clinker is partially replaced by a different constituent such as calcium carbonate, pozzolan, fly-ash, blast-furnace slag, etc. The content of supplementary constituent usually ranges between 18 and 30% of the cement, but the European standard EN 197-1 "Composition, specifications and conformity criteria for common cements" [1] allows the introduction of higher amounts. Pozzolan, fly-ash, blast-furnace slag, silica-fume exert hydraulic action in combination with Portland cement clinker, leading to cements with improved durability properties as high resistance to water aggression, sulfate and chloride attacks, carbonation reaction, etc.

Many new supplementary constituents have been proposed in the last years [2]: they usually derive from waste of different nature (ground glass [3,4], matt waste [5,6], rice husk ash [7], municipal solid waste incinerator bottom ash [8,9], ferroalloy industry waste [10,11], ceramic sludge [12], etc.). Their introduction in cement production aims to reach energy and costs saving, conservation of natural and not renewable resources, environmental protection with less waste landfill disposal, etc. Moreover, the performances of new constituents strongly depend on their average size and chemical/mineralogical composition: materials with high content of silica in the amorphous state and average dimension <10 μm may exhibit an active role in cement hydration reactions thus contributing in mechanical strength development, usually at long curing time.

Recently, polishing residue (PR), coming from porcelain stoneware tiles production, was successfully investigated as new constituent for innovative blended cement [12]. PR is the solid part of the relevant sludge formed during porcelain stoneware polishing step. This operation is performed on fired tiles by abrasive devices made of silicon carbide (SiC) and magnesium-based (MgOHCl) binder. In Europe, polishing sludge is classified as not hazardous waste (European Waste Code 10.12.99), but the presence of some compounds (CaO, MgO, SiC and chlorine compounds coming from the abrasive tools) prevents sludge re-introduction into the ceramic production cycle compromising a closed loop recycling. Italy (the 3rd world tile producer [13]) disposes to landfill more than 20,000 ton of polishing sludge every year.

In the previous work [12], mortar samples prepared with PR based blended cement, made up by 75 wt.% of CEM I 52.5 R and 25 wt.% of PR, exhibited good mechanical properties and compact microstructure due to the formation of calcium silicate hydrate (C-S-H) and K-rich-alumino-silicate-hydrate (K-A-S-H) gel structures. PR chemical/pozzolan activity towards portlandite was ascertained by different analytical characterizations (thermal analysis, scanning electron microscopy and EDS analysis), however durability tests were not carried out on the investigated binder.

It is commonly accepted in international standards and national laws that durability assessment is one of the most important issues for a building material and cement choice that can play a very important

* Corresponding author. Fax: +39 051 2090322.
E-mail address: maria.bignozzi@unibo.it (M.C. Bignozzi).

0008-8846/$ – see front matter © 2011 Elsevier Ltd. All rights reserved.
doi:10.1016/j.cemconres.2011.05.001

role for avoiding degradation processes. Investigations on degradation resistance are then required especially for those blended cement recently set up and/or introduced in the construction market. Accordingly, the aim of this research is to investigate the performances of mortar samples prepared with PR based blended cement when they are exposed to aggressive surroundings such as marine environment. The durability behavior has been studied by means of corrosion resistance measurements of steel reinforced mortar samples with the goal to assess if the performances of PR based mortar are comparable or better than that of mortar prepared with ordinary Portland cement (OPC). Half cell potential measurements, accelerated corrosion test by impressed voltage technique, linear polarization resistance experiments have been carried out on steel reinforced mortar samples cured up to 1 year and prepared using 75 wt.% of CEM I 52.5 R + 25 wt.% of PR or 100 wt.% of CEM I 52.5 R as binder. Moreover, after corrosion tests, chemical and physical parameters (chloride% and pH) as well as pore size distribution have been determined for the different mortar samples. The results are reported and discussed, highlighting the behavior of the two types of binders investigated under exposure to a chloride-rich environment.

2. Experimental procedure

2.1. Materials

The porcelain stoneware polishing residue (PR) is the solid part of relevant sludge coming from a specific multi-plants collecting landfill site (S.A.T. S.p.A. Service for the Environment, Sassuolo, Modena, Italy). After drying the sludge at T = 105 °C for 24–36 h, the solid part was ground and the fraction >0.106 mm eliminated by sieving. The resulting material has an average size of 8 μm, specific surface aerea of 25.9 m^2/g (by BET analysis Micromeritics Gemini Series, 2360 with N_2 at 77 K) and the chemical composition reported in Table 1. From a mineralogical point of view, PR is mainly constituted by quartz, mullite and albite calcian, deriving from porcelain stoneware body. Amorphous SiO_2 phase, traces of calcite and silicon carbide, deriving from the abrasive tools, were also determined. A complete chemical–physical characterization of PR is reported elsewhere [12].

CEM I 52.5 R (EN 197-1, Italcementi, Calusco d'Adda (BG) Italy) was used as ordinary Portland cement (specific surface aerea = 0.4 m^2/g) and silica sand, with normalized grain size distribution according to EN 196-1 [14], was used as aggregate. Steel bars (B450C) with a 6 mm diameter were used as reinforcement.

2.2. Sample preparation

Binder samples were prepared by dry mixing 25 wt.% of PR and 75 wt.% of CEM I 52.5 R: the amount of PR was set on the basis of compositional range of CEM II blended cement as reported in EN 197-1. Mixing procedure was carried out in a mixer for 30 min to ensure a repeatable mix. Reference binder was 100% OPC CEM I 52.5 R. Chemical (chloride and sulfate content) and physical (initial setting time and soundness) parameters of the PR based binder were previously determined [12] to ascertain the fulfilling of cement requirements set by EN 197-1: the data, collected in Table 2, are compared with those of 100% OPC.

Mortar samples were prepared by Hobart mixer according to the normalized mix-design (binder, sand and water in a weight ratio 1:3:0.5) reported in EN 196-1. Cylindrical samples (h:100 mm, d: 45 mm) with a 140 mm length reinforcing steel bar centrally embedded were prepared, as schematically reported in Fig. 1. Before mortar casting, the steel bars were cleaned with a wire brush and coated for 80 mm with an anticorrosion epoxy coating (Top-Armatec 108, Sika). The mold was filled in two steps using a vibrating table for compaction (vibration time about 1 min). Immediately after the cylindrical mold was filled, the steel bar was inserted into the mortar, such that its end was at least 20 mm from the bottom of the cylinder. The coated part remains for 20 mm inside the mortar sample (Fig. 1a) in order to avoid crevice corrosion at the top surface of the cylinder. Mortar samples were de-molded after 24 h and cured for different times (12, 28, 90, 120, 365 days) at R. H. >95% and T = 20 °C. Before corrosion tests, the bottom base of each cylinder was coated by a paraffin layer (Fig. 1a) thus allowing ions diffusion process only from the surrounding surfaces [15].

Mortar samples have been named M, followed by CEM or PR according to the binder used in the mix design and, when necessary, by a number indicating the curing time (e.g. MPR-12 is the mortar prepared with PR based binder, cured for 12 days at R. H. >95% and T = 20 °C).

2.3. Conditioning process and corrosion tests

After curing at R. H. >95% and T = 20 °C (standard condition), corrosion tests have been carried out in different laboratory conditions. Table 3 resumes the conditioning processes before and during corrosion measurements. Corrosion resistance of reinforced mortars MCEM and MPR was evaluated by means of electrochemical tests with the aim to compare durability behavior of PR based blended cement with OPC one.

Half cell potential (HCP) test was carried out on samples cured for 12, 28 and 90 days in standard condition and then exposed to drying and wetting cycles in two different environments: water and 3.5% NaCl solution. The reinforced samples were soaked in the solutions, taking care to keep 90 mm of the cylindrical sample immersed during the test. With the purpose to accelerate steel bar corrosion, all the specimens were exposed to 7 days of drying at room conditions, T ≈ 25 °C and R. H. ≈ 60%, and 7 days of wetting, soaked in the testing solutions. Corrosion activity was monitored after each cycle for 12 cycles (about 6 months) by means of a high impedance voltmeter (AT410 Tecnotest) connected to the reinforcing bar and a copper/copper sulfate electrode as reference. HCP test is considered a rapid indicator and a non-destructive test to evaluate steel bar corrosion activity: threshold values of electrical potential, established by ASTM C876 [16], are the following: E ≥ −0.2 V indicates very low probability

Table 1
Chemical composition of PR.

	wt.%
SiO_2	62.19
Al_2O_3	15.75
MgO	6.75
Na_2O	3.71
K_2O	1.46
CaO	2.24
ZrO_2	1.19
Fe_2O_3	0.59
ZnO	0.12
TiO_2	0.34

Table 2
Physical properties of the investigated binders (average of 2 measurements). Limits set by EN 197-1 are also reported.

Binder		Initial setting time[a] (min)	Soundness[a] (mm)	Cl^-[b] (wt.%)	SO_3[b] (wt.%)
CEM I 52.5 R		107	0.2	0.04	0.65
75% CEM I 52.5 R + 25% PR		105	0.2	0.09	0.51
Limits set by EN	32.5 R	≥75	≤10		
197-1 for cement	42.5 R	≥60		≤0.10	≤3.5
	52.5 R	≥45			

[a] Determined according to EN 196-3.
[b] Determined according to EN 196-2.

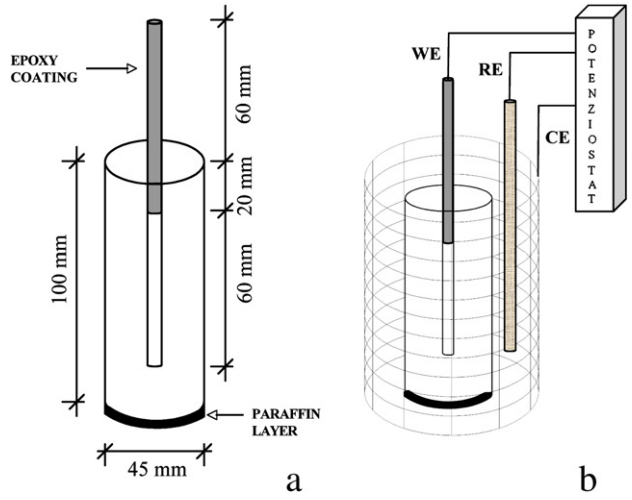

Fig. 1. Scheme of the sample (a) and measurement set-up (b).

of corrosion, $-0.35 \leq E < -0.2$ V indicates that corrosion state is uncertain, $E < -0.35$ V means very high probability (>90%) of corrosion.

Impressed voltage (IV) technique is an accelerated corrosion test that can be useful to get information about permeation characteristics of the matrix embedding steel reinforcement. After the preliminary curing, the sample was immersed in a 3.5% NaCl solution surrounded by a galvanized steel cage (Fig. 1b): steel bar (working electrode, WE), galvanized steel cage (counter electrode, CE) and $Hg/HgCl_2$ electrode (saturated calomel electrode, SCE, as reference, RE) were connected (3-electrode system) to a potenziostat (Potenziostat 7050 Amel Instrument). A constant voltage of 3 V was applied by the external DC source between the reinforcement (anode) and galvanized steel cage (cathode) with 3.5% NaCl solution working as electrolyte. Anodic current versus time plots at room temperature ($T = 25 \pm 1$ °C) were recorded and IV test was continued up to the occurrence of visual evidences of corrosion on the surface of the investigated sample.

Linear polarization resistance (LPR) technique was used to evaluate steel corrosion current intensity, I_{corr}, according to Stern–Geary relationship (Eq. (1)) [17]:

$$I_{corr} = B / R_p \quad (1)$$

where B is a constant determined by anodic and cathodic Tafel slopes β_a and β_c by Eq. (2) and R_p is the polarization resistance, that is the ratio between the potential shift ΔE and the corresponding current change ΔI in an experimental polarization test within a few millivolts (±20–25 mV) of the corrosion potential (E_{corr}) [15,18].

$$B = \frac{\beta a \beta c}{2.303(\beta a + \beta c)} \quad (2)$$

As proposed by different authors [14,17–19], for active state steel in concrete a B value of 26 mV can be adopted. A controlled potential scan, $E_{corr} \pm 0.020$ V, was applied with a scan rate of 0.17 mV/s to the reinforcing steel of mortar sample and the resulting current was plotted against the potential. R_p was determined by a curve-fitting method.

IV test was carried out on samples cured for 12, 28, 90, 120 and 365 days at R. H. >95%, T = 20 °C and then immersed in 3.5% NaCl solution. LPR measurements were carried out at the end of IV test.

Table 3
Curing condition and testing program for mortar samples (details of conditioning process and corrosion testing frequency are reported in Section 2.3).

Sample code	Initial curing condition (time)	Corrosion test
MCEM-12	12 days	HCP
MCEM-28	28 days	HCP
MCEM-90	90 days	HCP
MPR-12	12 days	HCP
MPR-28	28 days	HCP
MPR-90	90 days	HCP
MCEM-12	12 days	IV, LPR (at the end of IV test)
MCEM-28	28 days	IV, LPR (at the end of IV test)
MCEM-90	90 days	IV, LPR (at the end of IV test)
MCEM-120	120 days	IV, LPR (at the end of IV test)
MCEM-365	365 days	IV, LPR (at the end of IV test)
MPR-12	12 days	IV, LPR (at the end of IV test)
MPR-28	28 days	IV, LPR (at the end of IV test)
MPR-90	90 days	IV, LPR (at the end of IV test)
MPR-120	120 days	IV, LPR (at the end of IV test)
MPR-365	365 days	IV, LPR (at the end of IV test)

2.4. Microstructure characterization

Microstructure characterization was carried out on mortar samples after the IV and LRP tests. Water-soluble chloride content and pH were determined on powdered mortar fragments obtained by cylinder specimens. About 8.00 g of ground mortar (100% passing at 0.106 mm sieve) were stirred for 2 h with 250 ml of boiling water, then filtered: the solution was titrated by $AgNO_3$ 0.1 N (potassium bichromate as indicator) and pH was measured by a 315i WTW digital pHmeter [20].

Pore size distribution measurements were carried out by mercury intrusion porosimeter (MIP, Carlo Erba 2000) equipped with a macropore unit (Model 120, Fison Instruments) on samples obtained by cylinder specimens. Porosimeter samples, about 1 cm^3, were cut by a diamond saw, dried under vacuum and kept under P_2O_5 in a vacuum dry box till testing.

3. Results and discussion

3.1. Corrosion tests results

Electrical potential measured after 12 wetting and drying cycles by HCP method is reported in Fig. 2 for MCEM and MPR cured at 12, 28 and 90 days. All the mortar samples submitted to wetting and drying cycles in water always exhibit a potential >−0.2 V, thus indicating very low probability of corrosion for the reinforcing steel bars. Mortar samples exposed to 3.5% NaCl solution show potential values < −0.35 V, highlighting a high probability of corrosion. In both environments, at the end of 12 cycles, steel reinforcements in MCEM and MPR exhibit similar electrical potential values thus indicating the same probability of corrosion.

However, recording the electrical potential at the end of each cycle for sample submitted to wetting and drying cycles in NaCl solution (Table 4), it has been observed that (i) for samples cured at 12 and 28 days, MPR shows potential values <−0.35 V 1 month (2 cycles) earlier than MCEM; (ii) for samples cured at 90 days, both MPR and MCEM exhibit potential values <−0.35 V after 9 wetting and drying cycles. The potential decrease below the −0.35 V threshold is experienced at earlier time by PR based mortar than MCEM when samples are cured up to 28 days, whereas both MPR-90 and MCEM-90 exhibit such decrease in the same cycle.

The current-time plots obtained by impressed voltage test for the reinforced samples MCEM and MPR are shown in Figs. 3 and 4 respectively, in the case of samples permanently immersed in 3.5% NaCl solution. Whereas HCP test is affected by a certain level of uncertainty and relevant results only express a corrosion probability, IV measurements give quantitative information about the actual occurrence of corrosion.

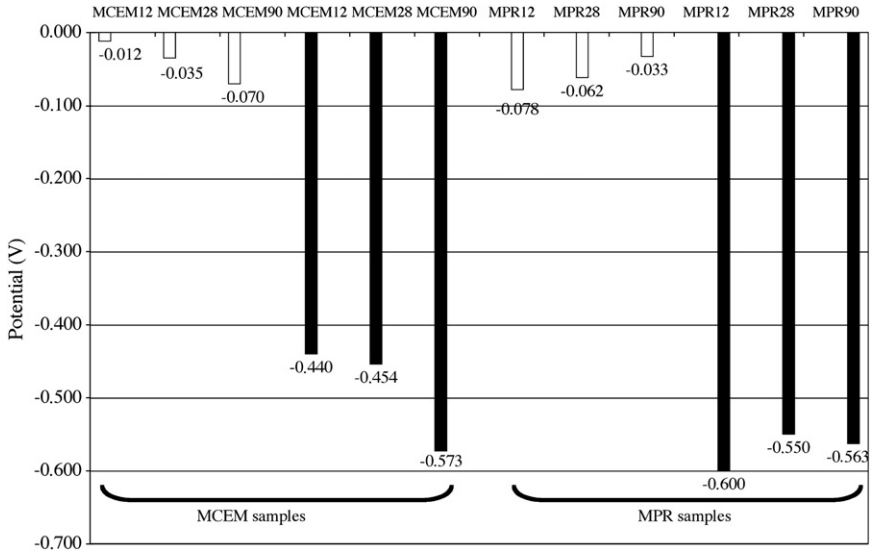

Fig. 2. HCP measurements (versus $Cu/CuSO_4$ electrode) after 12 drying and wetting cycles for MCEM and MPR samples cured at different times (empty bars refer to wetting and drying cycles in water, black bars refer to wetting and drying cycles in 3.5% NaCl solution).

Table 4
Half cell potential values for samples exposed to drying and wetting cycles in 3.5% NaCl solution (potential value in gray box indicates high probability of corrosion).

	Electrical Potential (V)											
N° of wetting/ drying cycles	1	2	3	4	5	6	7	8	9	10	11	12
MCEM–12	–0.23	–0.27	–0.25	–0.19	–0.21	–0.22	–0.42	–0.45	–0.48	–0.45	–0.46	–0.44
MPR–12	–0.27	–0.29	–0.25	–0.21	–0.61	–0.59	–0.61	–0.59	–0.59	–0.60	–0.61	–0.60
MCEM–28	–0.15	–0.14	–0.13	–0.14	–0.23	–0.25	–0.41	–0.39	–0.42	–0.37	–0.38	–0.45
MPR–28	–0.27	–0.25	–0.22	–0.24	–0.44	–0.49	–0.55	–0.51	–0.53	–0.53	–0.55	–0.55
MCEM–90	–0.18	–0.23	–0.21	–0.21	–0.25	–0.27	–0.29	–0.29	–0.43	–0.51	–0.53	–0.57
MPR–90	–0.21	–0.24	–0.24	–0.27	–0.25	–0.29	–0.28	–0.30	–0.45	–0.49	–0.54	–0.56

characterized by an initial decrease in current versus time, can be ascribed to the formation of iron oxide layer which initially slows down the corrosion phenomena. Such a decrease is more evident for 365 days, accordingly with the steel bar passivation spontaneously induced by the alkaline cement environment. After reaching constant current values (second step), the current suddenly increases when the

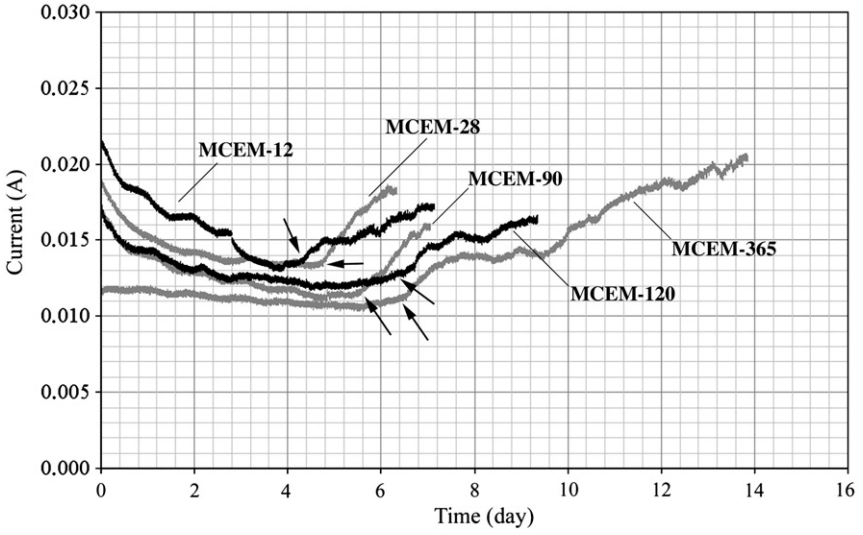

Fig. 3. Current-time plot at constant voltage of 3 V of reinforcing steel bar embedded in 100% OPC mortar samples at different curing time (the time of first crack, t_{fc}, is indicated by a black arrow for each curve).

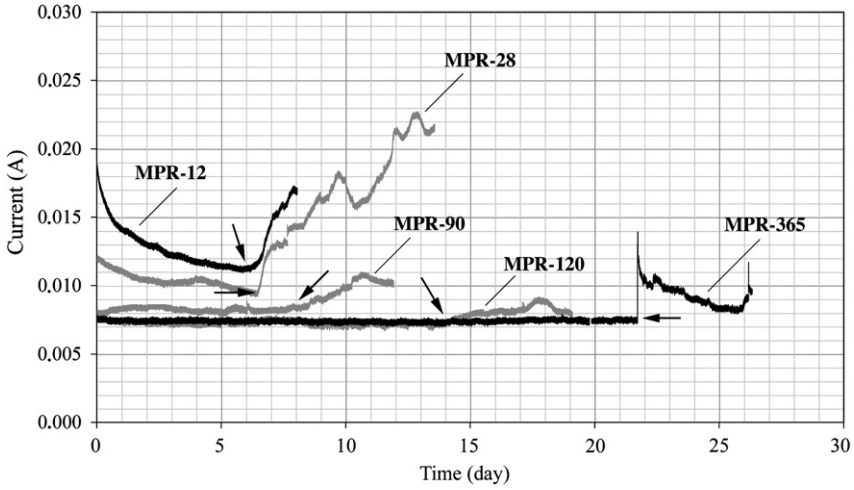

Fig. 4. Current-time plot at constant voltage of 3 V of reinforcing steel bar embedded in PR based blended cement mortar samples at different curing time (the time of first crack, t_{fc}, is indicated by a black arrow for each curve).

formation of micro-cracks in mortar samples occurs due to steel corrosion (third step). The time corresponding to the current increase has been named as the time of first crack (t_{fc}) and is indicated by an arrow for each sample in Figs. 3 and 4. Reporting t_{fc} for MCEM and MPR samples as function of curing time (Fig. 5), some observations can be as follows: (i) regardless the binder used, t_{fc} increases with mortar curing time according to a more compact microstructure obtained by the completion of binder hydration reactions; (ii) at 12 and 28 curing days, t_{fc} for MPR is slightly higher than that of MCEM, however such a difference increases as the curing time increases; (iii) t_{fc} trend can be interpolated: logarithmic and linear trends with correlation coefficients equal to 0.92 and 0.94 have been determined for MCEM and MPR samples respectively. Whereas t_{fc} does not change after 120 days of curing for MCEM, a linear increase is experimentally observed for MPR.

These results highlight how much curing time is important to improve corrosion resistance. They also show the added value that can be reached when PR based blended cement is used. The IV data quantify corrosion behavior of MPR and MCEM. With the increasing of mortar curing time, time of first crack for MPR becomes longer than that of MCEM, due to the development of a very compact microstructure for PR based mortar, thus involving a slow corrosion rate.

On mortar samples, visual evidences of corrosion appeared in the form of brown stains on side surface area and longitudinal cracks

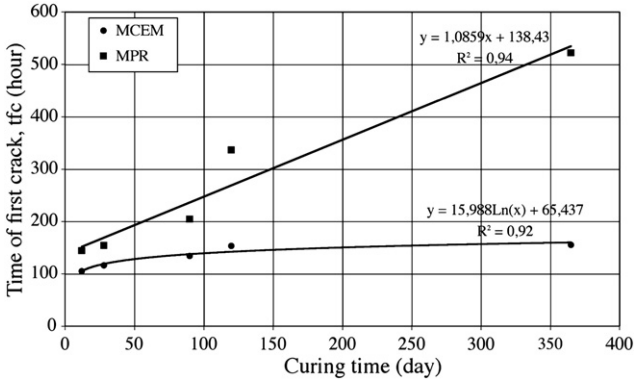

Fig. 5. Time of first crack (t_{fc}) as function of curing time for MCEM and MPR mortar (continuous line are logarithmic and linear trends respectively).

formation (Fig. 6a–b), and/or as brown stains on top surface area and steel bar epoxy coating destruction (Fig. 6c). Corrosion attack depends on the binder used for mortar preparation, as reported in Table 5. MPR samples, cured up to 28 days, show corrosion evidences on the side and top surface area, whereas at longer curing time corrosion preferentially starts on top surface area. A different behavior is exhibited by MCEM samples where corrosion always starts from side surface area. These results are very interesting as they seem to indicate that PR based binder is less permeable to chloride diffusion than OPC and such permeability becomes lower and lower as curing time increases. Corrosion evidences on side surface area are surely induced by chloride ion migrations from the solution into mortar sample, whereas corrosion evidences on the top surface area are probably due to the development of a differential aeration cell occurring on the reinforcement due to some crevices between bar and mortar. In this case corrosion leads to the destruction of the epoxy coating, without creating any longitudinal crack on mortar sample. As a further proof, MPR-90, MPR-120 and MPR-365 samples were sectioned and analyzed after corrosion test. Excluding the top surface where corrosion occurred, the deeper cross sections did not show any crack in the PR based matrix and no sign of corrosion was observed on the cross section of the steel bar.

Table 5 reports the total time required for IV test (it lasted up to visual evidences of corrosion as reported above) and corrosion current intensity (I_{corr}) of the reinforcement determined by LPR after IV test. OPC based mortar (MCEM) exhibits an I_{corr} ranging between 97 and 121 μA: such values correspond to a corrosion rate (CR) of 100–125 μm/year (exposed area: 11.3 cm^2, density: 7.8 g/cm^3, equivalent weight: 27.92). For PR based mortar, MPR-12 shows an $I_{corr} = 96$ μA corresponding to a CR = 99 μm/year. MPR-12 exhibits a slightly lower corrosion rate than MCEM-12. MPR samples cured for time ≥28 days exhibit a corrosion current intensity ranging between 24 and 37 μA and a relevant corrosion rate ranging between 25 and 38 μm/year. This indicates that, for curing time ≥28 days, PR based binder leads to a much better corrosion resistance of the steel reinforcement than that promoted by OPC. The determined corrosion rate is consistent with literature data that report CR values between 100–500 and 10–50 μm/year respectively for concrete highly contaminated by chloride with R. H. >95% and moderately contaminated by chloride with R. H. >85% [21].

For MPR-90, MPR-120 and MPR-365, CR data also agree with the specific corrosion evidences observed (Fig. 6c). The compact microstructure of PR based matrix acts as a very good protection barrier of

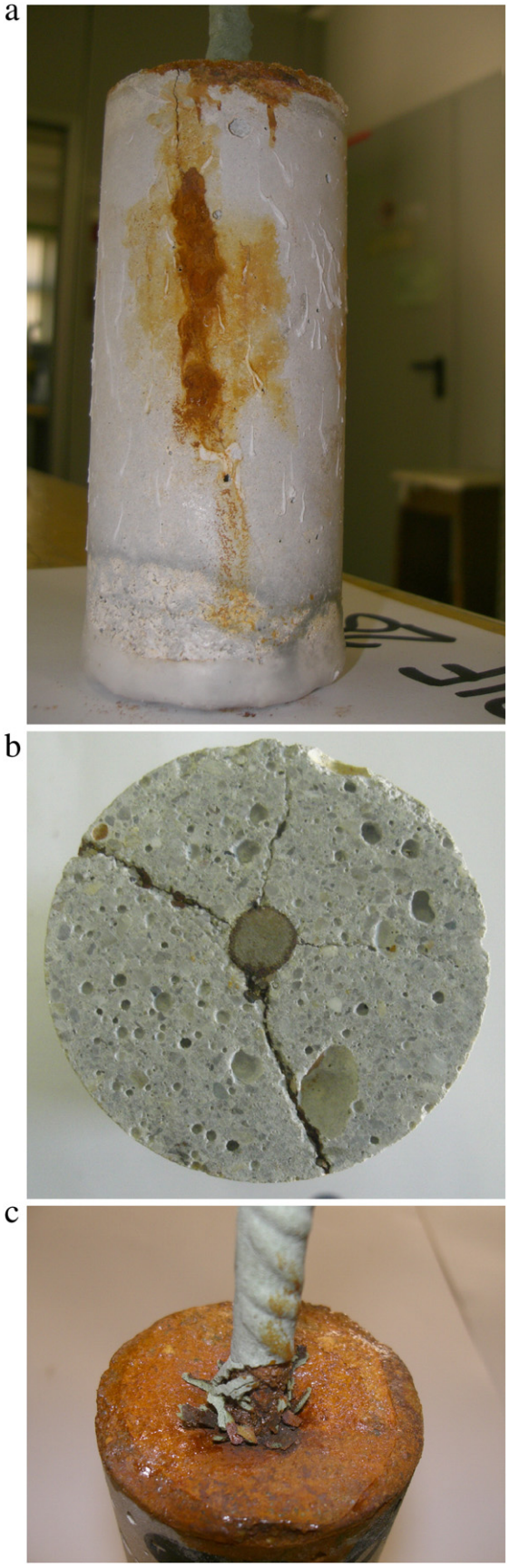

Fig. 6. Typical corrosion evidences and cracks formation after IV test on mortar: (a) brown stains and longitudinal crack on side surface area; (b) planar section of the longitudinal cracks; (c) brown stains on top surface area with steel bar epoxy coating destruction.

Table 5
Corrosion data for the investigated samples at the end of IV test.

Sample	Corrosion attack on		t_{fc}[a] (day)	IV test duration (day)	I_{corr}[b] (μA)	CR[c] (μm/year)
	Side surface area	Top surface area				
MCEM-12	yes	no	4.4	7.0	117	121
MCEM-28	yes	no	4.8	6.3	97	100
MCEM-90	yes	no	5.6	7.0	121	125
MCEM-120	yes	no	6.4	9.5	99	103
MCEM-365	yes	no	6.5	13.8	120	124
MPR-12	yes	yes	6.0	8.0	96	99
MPR-28	yes	yes	6.4	13.5	37	38
MPR-90	no	yes	8.5	12.0	30	31
MPR-120	no	yes	14.0	19.0	24	25
MPR-365	no	yes	21.8	26.2	36	37

[a] By IV test.
[b] By LPR after IV test.
[c] Exposed area: 11.3 cm^2, density: 7.8 g/cm^3, equivalent weight: 27.92.

steel reinforcement thus avoiding the formation of longitudinal cracks on the lateral surface area of the sample.

3.2. Microstructure test results

Pore size distribution, determined by MIP, is reported in Figs. 7 and 8 for MCEM and MPR samples, respectively. MIP test was carried out on samples obtained by cylinder specimens after IV and LRP measurements. Cumulative pore volume and mean pore radius are collected in Table 6 for the investigated samples.

MCEM and MPR samples exhibit pore size distributions that become smaller with the increasing of curing time. Accordingly, the cumulative pore volume lowers when increasing curing time from 12 to 365 days.

MCEM-12 and MCEM-28 exhibit smaller cumulative pore volume and larger mean pore radius than MPR-12 and MPR-28 samples, MCEM-120 shows a similar cumulative pore volume and larger mean pore radius than MPR-120, whereas MCEM-365 exhibits higher values for both parameters than MPR-365. In cement based materials mean pore radius, defined as the pore radius at which 50% of the pore volume was intruded in the pore size range considered, has similar value to the critical pore radius [22,23]. Since the last one corresponds to the smallest pore size diameter of the subset of the largest pores which creates a connected path through the sample, mean pore radius/critical pore radius has a direct influence on the transport properties, such as diffusion process. If a steel reinforced mortar is immersed in 3.5% NaCl solution, the mortar is saturated by the solution and, thanks to diffusion processes, a gradient of Cl^- occurs between the solution and the reinforcement. Since the chloride ions transport linearly increases with the mean pore radius, its size is strictly related to the corrosion behavior of the steel bar.

The lowest values of mean pore radius detected for MPR samples thus agree with the lowest corrosion rate determined by electrochemical tests. Such values further decrease with mortar curing time. Moreover, for MPR-120 and MPR-365 a refinement of pore size distribution is clearly evident (Fig. 8), especially for pore dimension $\leq$0.1 μm that is the pore dimension usually associated with cement paste capillary porosity.

The noteworthy refinement of pore size distribution with curing time for mortar prepared with PR based binder agrees with the porosity trend previously investigated on PR based mortar, thus confirming the chemical/pozzolan activity of PR [12].

Chloride content and pH values, determined on MCEM and MPR after electrochemical tests, are reported in Table 6. For all the investigated samples, pH values range between 11.5 and 11.8, just below the limit (12.0) for steel de-passivation in concrete. Chloride concentration, calculated as total Cl^-% over the binder content, ranges between 1.6 and 2.1% for OPC based mortar (MCEM), 1.0–1.5% for PR

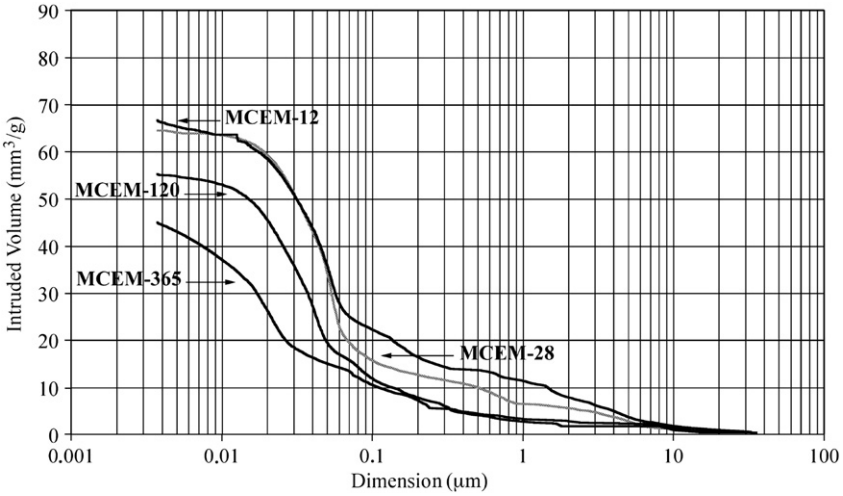

Fig. 7. Pore size distribution of MCEM samples at different curing time after IV and LRP tests.

based mortar cured up to 28 days and 0.4–0.7% for PR based mortar cured for time longer than 28 days.

Due to their smaller mean pore radius, MPR samples are then less permeable to chloride ions diffusion than MCEM. Curing time plays a very important effect when PR is used as binder constituent: the refinement of pores size, especially for those with dimension $\leq 0.1\,\mu m$, and small mean pore radius lead to a very compact microstructure less permeable to chloride ions and able to delay the beginning of degradation process of steel reinforcement.

Chloride ions diffusion is also related to the percolation path in the samples as well as electrokinetic phenomena occurring in the saturated pores. The finer the pores, the stronger the attractive forces between chloride ions and cement matrix are, thus leading to a noteworthy decrease of Cl^- diffusion process and corrosion rate. These features explain why samples showing a similar total porosity (e.g. MCEM-120 and MPR-120 in Figs. 7 and 8) have a different behavior in terms of Cl^- content [24–26].

According to the ranking system to establish corrosion activity based on chloride content (expressed as wt.% of cement) [15], it is possible to distinguish three levels: low corrosion state when $Cl^- < 0.3\%$, moderate corrosion state when $0.3 \leq Cl^- < 1\%$ and high corrosion state when $Cl^- \geq 1$. From the obtained data, all MCEM samples after IV and LRP tests are in a high corrosion state, whereas MPR samples are in moderate corrosion state except for MPR-12. The corrosion rate calculated by LRP agrees with the chloride content data: MPR120 and MPR-365 exhibit CR values that are about 1/3 of the relevant samples prepared with OPC and are characteristic of concrete moderately contaminated by chloride ions.

4. Conclusions

Based on the electrochemical tests and microstructure analysis carried out, the following conclusions can be drawn by the present study:

- half cell potential test highlights an important effect of curing time on the development of corrosion probability for polishing residue based mortar submitted to wetting and drying cycles in 3.5% NaCl solution. Under this experimental condition, polishing residue based mortar and ordinary Portland cement mortar experience their potential decrease below the −0.35 V threshold in the same cycle (thus indicating high corrosion probability) only if samples have been cured for ≥ 90 days.
- impressed voltage and linear polarization resistance data, determined on samples permanently immersed in 3.5% NaCla solution, show that polishing residue based mortar exhibits a better corrosion resistance (long time of first crack, low corrosion rate)

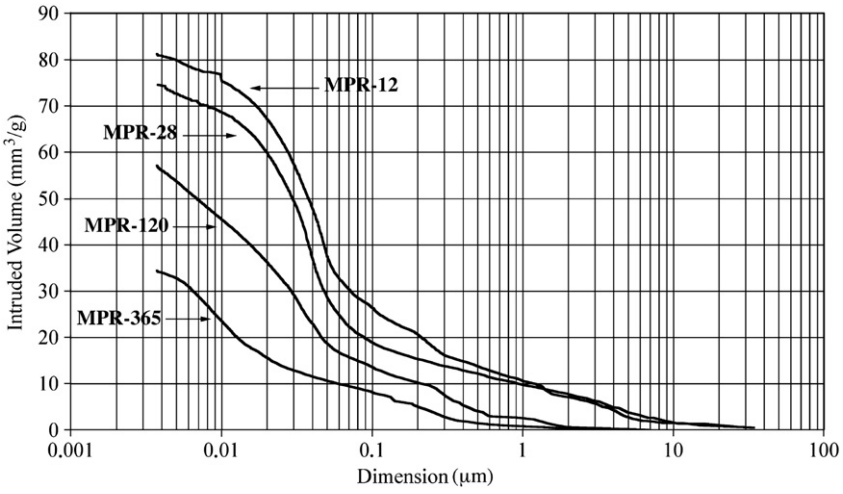

Fig. 8. Pore size distribution of MPR samples at different curing time after IV and LRP tests.

Table 6
Chemical–physical data for the investigated samples at the end of IV test.

Sample	IV test duration (day)	Comulative pore volume[a] (mm^3/g)	Mean pore radius[a] (μm)	$\%Cl^{-}$[b,c]	pH[c]
MCEM-12	7.0	66.6	0.053	2.1	11.5
MCEM-28	6.3	64.5	0.052	1.6	11.5
MCEM-120	9.5	55.2	0.039	1.6	11.8
MCEM-365	13.8	44.9	0.024	1.7	11.7
MPR-12	8.0	81.2	0.047	1.6	11.5
MPR-28	13.5	74.5	0.040	1.0	11.6
MPR-120	19.0	57.0	0.032	0.4	11.7
MPR-365	26.2	34.3	0.017	0.7	11.7

[a] By MIP.
[b] % over the binder content.
[c] Average of two measurements.

compared to that one of traditional OPC mortar. Such a behavior becomes more and more evident as the mortar curing time increases. Corrosion evidences, directly observed on samples surface, agree with the experimental data;
– MIP and Cl^{-}% analysis confirm that polishing residue based cement leads to the formation of microstructure characterized by smaller mean pore radius that influences interconnected pores size and, consequently, chloride diffusion governing corrosion processes. Curing time strongly contributes to pore size distribution refinement for polishing residue based mortar.

As final remark, blending polishing residue with ordinary Portland cement, in the investigated amounts, has significant influence on the hardened matrix, that becomes less permeable and porous, thus allowing the formation of a better protective barrier on steel reinforcement. As a consequence, polishing residue based blended cement have better durability performances than traditional OPC, mainly for curing time >28 days. Furthermore, electrochemical tests such as impressed voltage and linear polarization resistance techniques are very effective tools to provide data that can be usefully correlated with microstructure analysis results.

References

[1] European standard EN 197-1 Composition, specifications and conformity criteria for common cements, CEN, Brussels, 2007.
[2] M.C. Bignozzi, The use of industrial waste for the production of new blended cement, in: A.K. Haghi (Ed.), Waste Management: Research Advances to Convert Waste to Wealth, Nova Science Publishers, New York (USA), 2010, Chapter 7.
[3] Y. Shao, T. Lefort, S. Moras, D. Rodriguez, Studies on concrete containing ground waste glass, Cem Concr Res 30 (2000) 91–100.
[4] C. Shi, Y. Wu, Y. Shao, C. Riefler, H. Wang, Characteristics and pozzolanic reactivity of glass powders, Cem. Concr. Res. 35 (2005) 987–993.
[5] M.C. Bignozzi, A. Saccani, F. Sandrolini, Matt waste from glass separated collection: an ecosustainable addition for new building materials, Waste Manage. 29 (2009) 329–334.
[6] M.C. Bignozzi, A. Saccani, F. Sandrolini, Chemical–physical behavior of matt waste in cement mixture, Constr. Build. Mater. 24 (2010) 2194–2199.
[7] K. Ganesan, K. Rajagopal, K. Thangavel, Rice husk ash blended cement: assessment of optimal level of replacement for strength and permeability properties of concrete, Constr. Build. Mater. 22 (2008) 1675–1683.
[8] K.L. Lin, D.F. Lin, Hydration characteristics of municipal solid waste incinerator bottom ash slag as a pozzolanic material for use in cement, Cem. Concr. Compos. 28 (2006) 817–823.
[9] A. Saccani, F. Sandrolini, F. Andreola, I. Lancellotti, L. Barbieri, A. Corradi, Influence of the pozzolanic fraction obtained from vitrified bottom ashes from MSWI on the properties of cementitiuos composites, Mater. Struct. 38 (2005) 367–371.
[10] M. Frı'as, C. Rodrı'guez, Effect of incorporating ferroalloy industry wastes as complementary cementing materials on the properties of blended cement matrices, Cem. Concr. Compos 30 (2008) 212–219.
[11] M. Frías, M.I. Sánchez de Rojas, C. Rodríguez, The influence of SiMn slag on chemical resistance of blended cement pastes, Constr. Build. Mater. 23 (2009) 1472–1475.
[12] F. Andreola, L. Barbieri, M.C. Bignozzi, I. Lancellotti, F. Sandrolini, New blended cement from polishing and glazing ceramic sludge, Int. J. Appl. Ceram. Technol. 7 (2010) 546–555.
[13] P. Giacomini, World production and consumption of ceramic tiles, Ceramic World Review 68 (2006) 58–76.
[14] European Standard EN 196-1 Methods of Testing Cement—Part 1: Determination of Strength, CEN, Brussels, 2005.
[15] H.R. Soleymani, M.E. Ismail, Comparing corrosion measurement methods to assess the corrosion activity of laboratory OPC and HPC concrete specimens, Cem. Conc. Res. 34 (2004) 2037–2044.
[16] American Standard ASTM C876 Standard Test Method for Corrosion Potentials of Uncoated Reinforcing Steel in Concrete, American Society for Testing and Materials, West Conshoshockner, PA, USA, 2009.
[17] M. Stern, A.L. Geary, Electrochemical polarization: I A theoretical analysis of the shape of polarization curves, J. of Electrochemical soc. 104 (1957) 56–63.
[18] Z.T. Chang, B. Cherry, M. Marosszeky, Polarisation behaviour of steel bar samples in concrete in seawater. Part 1: experimental measurement of polarisation curves of steel in concrete, Corros. Sci. 50 (2008) 357–364.
[19] C. Andrade, J.A. González, Quantitative measurements of corrosion rate of reinforcing steels embedded in concrete using polarisation resistance measurements, Werkst. Korros. 29 (1978) 515–519.
[20] J. Flis, S. Sabol, H.W. Pickering, A. Sehgal, K. Osseo-Asare, P.D. Cady, Electrochemical measurements on concrete bridges for evaluation of reinforcement corrosion rates, Corrosion 49 (1993) 601–613.
[21] B. Hans, Corrosion in Reinforced Concrete Structures, Woodhead Publishing, Cambridge, UK, 2005.
[22] P. Halamiclova, R.J. Detwiler, D.P. Bentz, E.J. Garboczi, Water permeability and chloride ion diffusion in Portland cement mortars: relationship to sand content and critical pore diameter, Cem Conc Res 25 (1995) 790–802.
[23] M.D. Roy, Relationship between permeability, porosity, diffusion and microstructure of cement paste, mortar and concrete at different temperature, in: L.R. Roberts, J.P. Skalny (Eds.), Pore Structure and Permeability of Cementitious Materials, Third Edition, Mater. Res. Soc. Symp. Proc. (Boston), vol. 137, 1988, pp. 179–189.
[24] P.S. Mangat, J.M. Khatib, B.T. Molloy, Microstructure, chloride diffusion and reinforcement corrosion in blended cement paste and concrete, Cem. Concr. Compos. 16 (1994) 73–81.
[25] B.F. Johannesson, A theoretical model describing diffusion of a mixture of different types of ions in pore solution of concrete coupled to moisture transport, Cem Conc Res 33 (2003) 481–488.
[26] P. Pivonka, C. Hellmich, D. Smith, Microscopic effects on chloride diffusivity of cement pastes—a scale-transition analysis, Cem Conc Res 34 (2004) 2251–2260.